The Astrophysical Journal, 501:L139–L144, 1998 July 1

PROBING THE SUBSURFACE STRUCTURE OF ACTIVE REGIONS WITH THE PHASE INFORMATION IN ACOUSTIC IMAGING

Huei-Ru Chen,[1] Dean-Yi Chou,[1] Hsiang-Kuang Chang,[1] Ming-Tsung Sun,[2] Sheng-Jen Yeh,[1]
Barry LaBonte,[3] and the TON Team[4]

Received 1998 February 4; accepted 1998 May 1; published 1998 June 18

ABSTRACT

We present the phase information of solar *p*-mode waves constructed with an acoustic imaging technique in the solar interior. There exists a phase shift between the time series constructed with ingoing waves and outgoing waves. We find that this phase shift is different in an active region and the quiet Sun. The *p*-mode travel time is shorter in the magnetic regions than in the quiet Sun. We construct a three-dimensional phase shift map of the solar interior. As with the acoustic absorption images, the phase shift features of the active region in maps at the surface correlate with magnetic fields. The vertical extension of phase shift features in the active region is smaller in the phase maps constructed with shorter wavelengths. This indicates the vertical spatial resolution of these three-dimensional phase maps is sensitive to the range of modes used in constructing the signal. The actual depths of the phase shift features in the active region may be smaller than those shown in the three-dimensional phase maps.

Subject headings: Sun: magnetic fields — Sun: oscillations — sunspots

1. INTRODUCTION

Recently, Chang, Chou, & LaBonte (1997, hereafter Paper I) developed a technique, acoustic imaging, based on the time-distance relation, to construct a three-dimensional acoustic intensity image of the solar interior with the helioseismic data taken with the Taiwan Oscillation Network (TON). A mathematical description of a related holographic imaging concept was independently developed by Lindsey & Braun (1997). Chou et al. (1998, hereafter Paper II) measured the cross-correlation between the constructed time series and the observed time series at the same surface point to quantify the success of acoustic imaging. They found that the phase of the time series constructed with the outgoing waves is ahead of the observed time series by about 1 minute and that the phase of the time series constructed with the ingoing waves is behind the observed time series by about 1 minute in the quiet Sun. In this study, we show that the relative phase between the time series constructed with ingoing and outgoing waves is different in the quiet Sun and in an active region. The sign of the difference indicates that the travel time is shorter in magnetic regions than in the quiet Sun. We construct three-dimensional phase shift maps of the solar interior for a region including the active region NOAA 7981 and the quiet Sun.

2. PRINCIPLE AND METHOD

A resonant *p*-mode is trapped and multiply reflected in a cavity between the surface and a layer in the solar interior. The acoustic signal emanating from a point at the surface propagates downward to the bottom of the cavity and back to the surface at a different horizontal distance from the original point. Different *p*-modes have different paths and arrive at the surface with different times and different distances from that point. The modes with the same angular phase velocity ω/l have approximately the same ray path, where ω is the mode frequency and l is the spherical harmonic degree.

The propagation of solar acoustic waves from a point $(\boldsymbol{r}, t)$ to another point $(\boldsymbol{r}', t')$ in spacetime can be described by a propagator (Lindsey & Braun 1997; Paper II)

$$G(\boldsymbol{r}, t;\ \boldsymbol{r}', t') \propto (\sin\Delta)^{-1/2}\delta(t' - [t + \tau]), \tag{1}$$

where τ is the travel time from $\boldsymbol{r}$ to $\boldsymbol{r}'$ and in general is a function of $\boldsymbol{r}$ and $\boldsymbol{r}'$, and Δ is the angular distance between $\boldsymbol{r}$ and $\boldsymbol{r}'$. The source point $\boldsymbol{r}$ can be any point on the solar surface or in the solar interior, and $\boldsymbol{r}'$ is the observing point on the surface. The Dirac delta function, corresponding to the time-distance relation (Duvall et al. 1993), can be computed from a standard solar model based on ray theory (Papers I and II). The *p*-modes emanating from $(\boldsymbol{r}, t)$ can be grouped into different wave packets characterized by the angular phase velocity ω/l. Different wave packets bounce back to the surface at different $(\boldsymbol{r}', t')$. If we collect the acoustic signals measured at all $(\boldsymbol{r}', t')$ based on the wave propagator in equation (1), we can reconstruct the acoustic wave amplitude at $(\boldsymbol{r}, t)$, which propagated outward from $\boldsymbol{r}$. In the practical analysis, the constructed signal at the target point at t, $\Psi_c(t)$, is the computed with (Paper II)

$$\Psi_c(t) = \sum_{\tau=\tau_1}^{\tau_2} \bar{\Psi}(\Delta, t + \tau) \cdot (\sin\Delta)^{1/2}, \tag{2}$$

where $\bar{\Psi}(\Delta, t + \tau)$ is the azimuthal-averaged signal measured at a distance Δ from the target point at time $t + \tau$, and τ and Δ follows the time-distance relation. The summation variable τ is evenly spaced in the interval (τ_1, τ_2). The factor $(\sin\Delta)^{1/2}$ is to compensate the decrease of wave amplitude. We

[1] Physics Department, Tsing Hua University, Hsinchu, 30043, Taiwan, R.O.C.
[2] Department of Mechanical Engineering, Chang-Gung University, Kwei-San, 33333, Taiwan, R.O.C.
[3] Institute for Astronomy, University of Hawaii, Honolulu, HI 96822.
[4] The TON Team includes: Heng-Tai Tang, Wei-Cheng Shiu, and Yi-Liang Chen (Physics Department, Tsing Hua University, Hsinchu, 30043, Taiwan); Antonio Jimenez and Maria Cristina Rabello-Soares (Instituto Astrofisica de Canarias, Observatorio del Teide, Tenerife, Spain); Guoxiang Ai and Gwo-Ping Wang (Huairou Solar Observing Station, Beijing Observatory, Beijing, China); Philip Goode and William Marquette (Big Bear Solar Observatory, New Jersey Institute of Technology, Newark, NJ 07102); Shuhrat Ehgamberdiev and Shukur Khalikov (Ulugh Beg Astronomical Institute, Tashkent, Uzbekistan).

can also construct the signal at ($\boldsymbol{r}$, t) from the waves propagating inward from the surrounding area if we use a time-reversed time-distance curve (replacing τ in eq. [2] by $-\tau$). The acoustic image constructed with the time-reversed time-distance curve does not show any signature of sunspots because the ingoing waves in the surrounding area have not been affected by the sunspots before reaching it (Papers I and II). It is noted that the constructed signal defined in equation (2) is different from the egression defined in Lindsey & Braun (1997). In our opinion, their egression and ingression do not lead to reconstructing the signal at the target point.

The time series of constructed amplitude includes both intensity and phase information. The intensity is computed by integrating the squared amplitude over time. One can form a three-dimensional intensity image of solar interior with the outgoing waves or the ingoing waves (Paper I). One can also form an absorption image by subtracting the ingoing intensity (constructed with the ingoing waves) from the outgoing intensity (constructed with the outgoing waves) and then dividing by the ingoing intensity (Paper II). The absorption images can be used to study the three-dimensional structure of the absorption of an active region below the surface. There exists a phase difference between the ingoing time series and the outgoing time series (Paper II). The relative phase between two time series can be determined from the cross-correlation, which is defined as equation (14) in Lindsey & Braun (1997), although our constructed time series defined in equation (2) are different from the egression and ingression defined in Lindsey & Braun. To study the phase change in the active region, we measure the phase shift between the time series constructed with ingoing and outgoing waves. This method is better than measuring the phase shift between the constructed time series and the observed series because it is difficult to accurately observe p-modes inside sunspots. Constructing the signal with outgoing waves or ingoing waves does not use the signal observed at the target point. This avoids the measurement problem inside sunspots discussed in Braun (1997).

One has to be cautious in measuring the phase shift between the ingoing signal and the outgoing signal. Since the acoustic waves are generated with random phases, if the observed ingoing signal and outgoing signal used to construct the wave amplitude at the target point are not the same wave packet, the measured phase shift is meaningless. We illustrate the problem in Figure 1. If the target point T lies on the surface, then Figure 1*a* shows the ray paths of ingoing and outgoing waves. The ingoing wave observed at A turns into the outgoing wave observed at B after reflecting at the target point T. Since we use the azimuthal-averaged signal to construct the amplitude at T, the signal constructed with the ingoing waves and the signal constructed with the outgoing waves are from the same wave train and may be used to measure a phase shift.

If the target point T is in the solar interior as shown in Figure 1*b*, the situation is more complicated. The ingoing waves with the same ω/l observed at A and B pass the target point T and turn into the outgoing waves observed at C and D, respectively. If one uses the signal observed at A to construct the ingoing amplitude at T and uses the signal observed at D to construct the outgoing amplitude at T, as we did in constructing the absorption images (Paper II), the phases of constructed ingoing and outgoing signals at T will have no correlation since they are different wave trains. In principle one may use the signal observed at C, which is the same wave train as that observed at A, to construct the outgoing signal at T. But in practice C may be so close to the target point T that two problems will arise. First, the number of observed data points near the target point is small, making the constructed signal inaccurate (Paper II). Second, if the target point is inside the sunspot, point C may be also inside the sunspot where the oscillatory signal cannot be accurately measured. Similarly, one cannot use the signal observed at B as ingoing waves and signal observed at D as the outgoing waves because B is too close to T, even though D is far enough from T. To circumvent these difficulties, we use the one-bounce ingoing waves observed at A, which is not too close to T, to construct the ingoing amplitude at T, and we use the two-bounce outgoing waves observed at E to construct the outgoing amplitude at T in equation (2). This requirement for measuring the same wave packet does not occur in the acoustic intensity measurement. We can even compare slightly different wave packets in making an absorption image so long as the absorption is a slow function of ω/l.

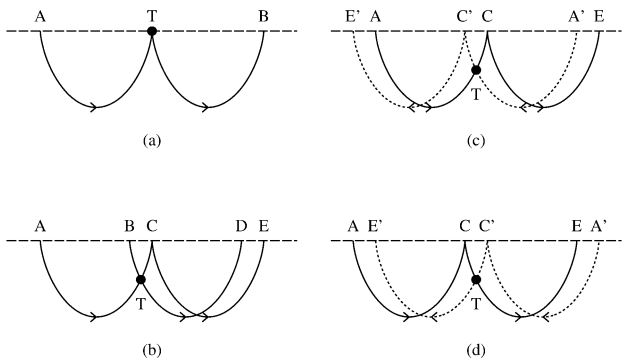

FIG. 1.—Sketch of the ray paths of waves with the same ω/l. The horizontal dashed line represents the solar surface. (*a*) The target point T is located at the surface. The ingoing waves observed at A arrive at T and turn into the outgoing waves observed at B. (*b*) The target point T is located in the solar interior. The ingoing waves observed at A pass T and turn into the outgoing waves observed at C after one bounce and at E after two bounces. Another ingoing waves with the same ω/l originating at B pass T and turn into the outgoing waves observed at D. (*c*) For each ray path ACE (*solid lines*) passing the target point T, there exits another ray path A′C′E′ (*dotted lines*) in our coherent summation because the signals are averaged over a ring centered at the target point. (*d*) Same path as (*c*), but with an opposite direction. ACE has the same path as A′C′E′ in (*c*), but they have opposite directions. Similarly, A′C′E′ has the same path as ACE in (*c*) but has an opposite direction.

3. RESULTS AND DISCUSSION

The helioseismic data used in this study were taken with the instruments of the Taiwan Oscillation Network (TON) in Tenerife, Big Bear, and Tashkent. A discussion of the TON project and its instruments is given in Chou et al. (1995). The time series in this study is 1996 August 1–3. The data coverage is about 82%. We select NOAA 7981 (the same region studied in Paper II), which is a large old active region, as the target region. The preceding sunspot has little change, while the several following sunspots change significantly during this period. The latitude of the preceding sunspot is about 10° south in the Carrington coordinates. The preliminary data reduction of the TON data, such as flat-fielding and registration, is given in Chen, Chou, & the TON Team (1996). The data reduction to construct the time series of ingoing and outgoing amplitudes at different focal depths is discussed in Paper II.

In this study, we use two different annular collecting areas (apertures), corresponding to different l ranges, to construct the acoustic signal at the target point. The small-angle aperture is 2°–5.°5, corresponding to $l = 202$–378 at 3 mHz for the surface.

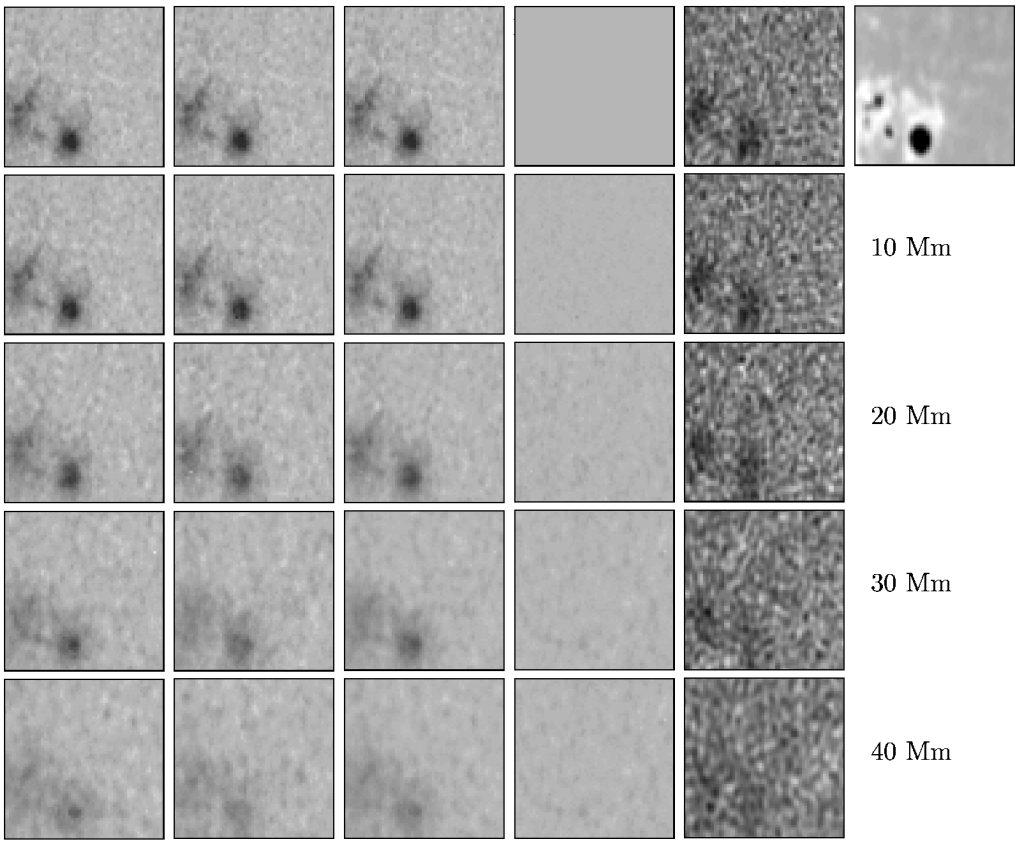

FIG. 3.—Phase shift maps at various focal depths (0, 10, 20, 30, and 40 Mm) for the large-angle aperture (2°–16°). The horizontal (ϕ) and vertical ($\sin\theta$) dimensions are 21°.1 and 13°.3, respectively. For comparison, the corresponding absorption images (derived from the same data set) are shown in the fifth column. The corresponding observed *K*-line image averaged over the same observing period is shown in the sixth column. The maps in the first column are constructed with the ray paths shown in Fig. 1*c*, and the maps in the second column are constructed with the ray paths shown in Fig. 1*d*. The maps of in third and fourth columns are mean and difference of maps in the first and second columns, respectively. The darkest point at the center of the sunspot at the surface corresponds to 1.1 minutes. The fluctuation of the quiet Sun in the mean maps is about 0.07 minutes.

The large-angle aperture is 2°–16°, corresponding to $l = 100$–378. In the measurements made using the small-angle aperture, we find that the intensity maps constructed by the ingoing waves show ghost images near the sunspots, which are caused by inaccurate signals measured in the sunspots (the observed signal in the sunspot is set zero in the data processing). Thus, we use two-bounce ingoing waves and three-bounce outgoing waves for the small-angle aperture to avoid the effect of sunspots.

The time series of wave amplitude constructed with ingoing and outgoing waves have a relative phase shift. To determine the phase shift, we computed the cross correlation function of two constructed time series and then fitted the cross correlation function with a Gabor wavelet,

$$G = A \cos\left(2\pi\nu[t - \tau_{\rm ph}]\right) \exp\left[-\frac{(t - \tau_{\rm en})^2}{2\sigma^2}\right], \qquad (3)$$

where A, σ, and $\tau_{\rm en}$ are the amplitude, width, and location of a Gaussian envelope, respectively, and ν is the modulation frequency. The typical value of A is about 0.5 for large-angle and 0.4 for small-angle. The average value of ν is 3.35 mHz, corresponding to a period of 4.98 minutes. The location of a modulation peak, $\tau_{\rm ph}$, is called the phase shift (time lag), which is defined such that a positive $\tau_{\rm ph}$ means that the phase of time series constructed with outgoing waves is ahead of that constructed with ingoing waves. In measurements with the large-angle aperture, the typical value of $\tau_{\rm ph}$ is about 2.6 minutes in the quiet Sun and about 3.2 minutes in the active region. The relative phase shift between two time series is computed for every point in a target region to form a phase map at a fixed focal depth. The data from each observing station on each day, defined as one unit, are analyzed separately to obtain a phase map. The phase maps derived from different units are consistent. The final phase map is the average over seven units in the period 1996 August 1–3. The same procedure is repeated for focal depths 0–80 Mm at intervals of 10 Mm for large-angle and 0–40 Mm for small-angle. The variation of phase shift in the quiet Sun is small (about 0.16 minutes for small-angle aperture and 0.07 minutes for large-angle aperture).

To study the phase shift caused by inhomogeneities in the active region, we use $\tau_{\rm qs}$ as the reference; namely, we are interested in $\tau'_{\rm ph} = \tau_{\rm ph} - \tau_{\rm qs}$ at each target point. The maps of $\tau'_{\rm ph}$ at various focal depths are shown in the first column of Figures 3 and 4. The absorption images at the same focal depths are shown in the fifth column (Paper II). The *K*-line intensity image averaged over the same observing period is shown in the sixth column. The average $\tau'_{\rm ph}$ over the quiet Sun is zero, and $\tau'_{\rm ph}$ is positive in the active region, indicating that *p*-modes have shorter travel times in the active region. Positive values of $\tau'_{\rm ph}$ are represented as darker for comparing with the absorption images.

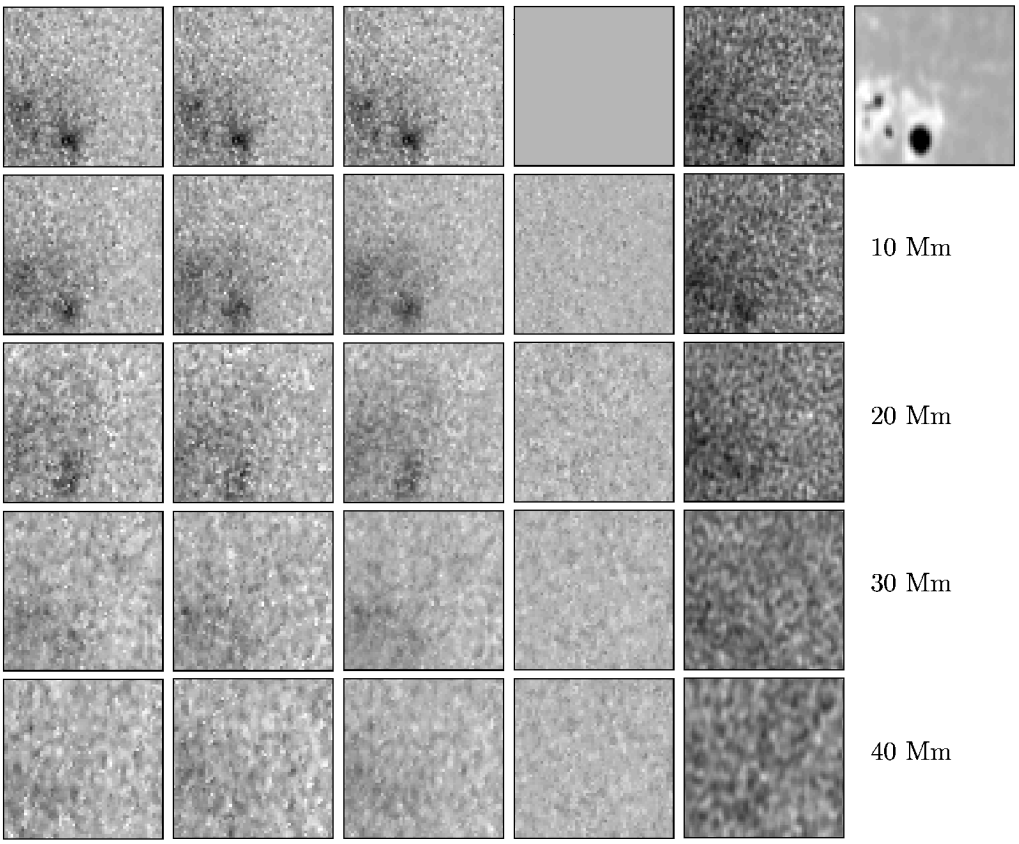

FIG. 4.—Same as Fig. 3 for the small-angle aperture (2°–5°5). The vertical extension of phase shift features in the active region is smaller than that of large-angle aperture. The phase shift features are sharper and noisier and have a smaller fluctuation length scale in the quiet Sun. The gray scale is the same as Fig. 3.

The phase shift $\tau'_{\rm ph}$ measured here could be caused by either a change in *p*-mode travel time or a change in conditions at boundaries of the mode cavity. If the ray path reaches the boundary in the magnetic region, a change in the boundary conditions will result in a change in phase jump at the boundary. The change in travel time could be caused by (1) mass flow, (2) thermal perturbations changing the sound speed, (3) modification of the acoustic cutoff frequency, and (4) magnetic fields along the ray path (Kosovichev & Duvall 1998). Only the first term changes the sign of time lag for rays propagating in opposite directions. The time lags from other three terms do not change sign for oppositely directed rays. Although the fourth mechanism depends on the angle between the wave vector and magnetic field, oppositely directed rays have the same time lag. In the active region, the second and third mechanisms are indirectly related to magnetic field. The change in boundary conditions is also indirectly related to magnetic field and independent of the direction of the ray path. Thus, all terms related to magnetic field do not change sign for waves traveling in opposite directions. Hereafter, we call the combined effects of all these mechanisms the magnetic term.

We first discuss the contribution of the flow term with the aid of Figure 1*c*. Similar to Figure 1*b*, in Figure 1*c* the ingoing signal observed at A passes the target point T and arrives at C after one bounce and at E after two bounces. We use the signal observed at A to construct the ingoing amplitude at T and use the signal observed at E to construct the outgoing amplitude at T. Since we use the azimuthal-averaged signal to construct the amplitude at T, for each ray path ACE, there exits another ray path A′C′E′ in our coherent summation. For the flow at T, our phase shift measurement picks up only its vertical component because the contributions of horizontal component for the ray paths ACE and A′C′E′ have opposite signs and cancel. For a target point on the surface, ACE and A′C′E′ are identical but have opposite directions. Thus, the flow has no contribution to $\tau'_{\rm ph}$. At deeper focal depths, $\tau'_{\rm ph}$ will be increasingly sensitive to mass flows.

To separate the contribution of the flow term from the magnetic term, we have to construct the wave amplitude at the target point separately from waves propagating opposite directions (Duvall et al. 1996). The ray paths in Figure 1*d* fulfill this purpose. The ray paths in Figure 1*d* have the same path as those in Figure 1*c*, but with opposite directions. The phase maps constructed with the ray paths in Figure 1*d* are shown in the second column of Figures 3 and 4. The flow term has opposite signs for the ray paths in Figures 1*c* and 1*d*, and the magnetic term has the same sign. Thus, the difference of the phase maps in the first and second columns has the contribution only from the flow term, while the mean of the two maps has the contribution only from the magnetic term. The mean maps and the difference maps at various focal depths are shown in the third and the fourth columns of Figures 3 and 4, respectively. It is noted that the phase shift shown in Figures 3 and 4 measures the travel time perturbation averaged over many different ray paths, because the wave amplitude at the target point in our study is constructed from the data over the entire annular aperture. These ray paths have different directions in three dimensions.

If the target point T is on the surface, the ray paths in Figures 1*c* and 1*d* are identical. Thus, the contribution of flow to the

difference map is zero at the surface and increases with focal depth. The difference maps in the solar interior have very small values and do not show any features in the active region. Its spatial rms value increases with focal depth and approaches the rms value of the mean map at about 20 Mm. There are several that limit the sensitivity of the difference map defined here for detecting mass flow in the active region. The difference maps cancel any flow signals at the surface. From mass conservation, we expect that the flow velocity decreases with depth. Thus, it is not a surprise that the difference maps do not show evidence of mass flow in the active region at any focal depth.

The mean maps defined here do remove the contribution of flow and show only the magnetic effects. We discuss several phenomena shown in the mean maps and differences between the small-angle and large-angle images here. (1) The phase shift $\tau'_{\rm ph}$ is positive in the active region. The correlation between the phase map at the surface and the *K*-line image is apparent. The positive $\tau'_{\rm ph}$ in the active region indicates that *p*-mode travel time is shorter in the magnetic region than that in the quiet Sun, as expected (Braun et al. 1992). The phase shift features have better correlation with surface magnetic field structures than the absorption features. One can even identify the correlation between the *K*-line image and the phase maps for some weak features in the quiet Sun in Figure 3. (2) The maximum phase shift occurs at the center of the preceding sunspot and is about 1.1 minutes at the surface. The phase shift in the active region decreases with focal depth. The phase shift averaged over the preceding sunspot at various focal depths is shown in Figure 2. (3) The phase shifts measured with the small-angle and large-angle apertures are nearly the same in the sunspot at the surface. But the small-angle shifts decrease with focal depth more rapidly than the large-angle shifts. This indicates the vertical spatial resolution of these three-dimensional phase maps is sensitive to the range of modes used in constructing the signal. The appearance of the phase shift features over a great range of focal depths in Figures 3 and 4 may be exaggerated over their true depths. Until the vertical resolution can be quantified, it is premature to identify the actual depth of the phase shift features in the active region based on these three-dimensional phase maps. Modeling of the acoustic imaging process may help solve this issue. (4) The phase maps made from the small-angle aperture are sharper and noisier and have a smaller fluctuation length scale in the quiet Sun. The sharpness and the smaller fluctuation scale are a result of the smaller wavelengths sampled. The greater noise may be caused by the lower power in the acoustic spectrum at small wavelengths and from incomplete cancellation of undesired modes over the small aperture. Another source of noise in phase shift is that the phase determination in the fit is sensitive to the noise in the time series. This may explain the larger increase in noise in the phase maps than in the absorption maps.

It is of interest to compare our results with other work. (1) Duvall et al. (1996) and Braun (1997) found a significant difference in travel times (phase time) between waves traveling in opposite directions, into and out from a sunspot. Their measurements were based on cross-correlation of the time series observed inside the sunspot and in the quiet Sun. From their measurement, Duvall et al. inferred a very small flow velocity if the flow persists to a deep layer. Because our difference map may only be able to detect a significant flow signal at depth, and because we have not yet quantified the relation between the flow velocity and our difference maps at various focal depths, we cannot determine if our result is consistent with the result of Duvall et al. (2) The perturbation of the two-bounce travel time (~0.65 minutes at 10°–15°) measured by Braun (1997) is consistent with our phase shift (~0.68 minutes) averaged over the umbra and penumbra at the surface, but smaller than our value (~1.1 minutes) at the center of the sunspot. If Braun's result is extrapolated to the range of 2°–16° in our large-angle aperture, it falls between 0.68 and 1.1 minutes. Note that, unlike the measurement in Duvall et al. (1996), we do not use the signals observed inside the sunspot, nor did Braun in his two-bounce measurement.

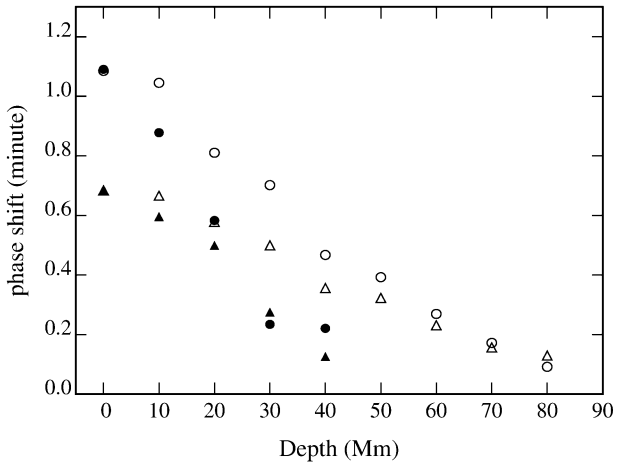

FIG. 2.—Phase shift $\tau'_{\rm ph}(\equiv \tau_{\rm ph} - \tau_{\rm qs})$ in the preceding sunspot at various focal depths. The open symbols denote the phase shifts of large-angle aperture, and the filled symbols denote the phase shifts of small-angle aperture. The circle is $\tau'_{\rm ph}$ averaged over 3 × 3 pixels at the center of the preceding sunspot. The triangle is $\tau'_{\rm ph}$ averaged over the umbra and penumbra of the preceding sunspot. The phase shifts of small-angle and large-angle apertures at the surface are nearly the same, so the corresponding open and filled symbols coincide.

From this study, we conclude that the phase of constructed acoustic signals probably is a better tool than the intensity to probe the subsurface structure of magnetic fields. First, the phase perturbation more directly relates to magnetic field. The phase shift mainly depends on the field strength, while the absorption strongly depends on the orientation of magnetic field (Bogdan & Braun 1995 and references therein). Second, the phase shift measurement is more sensitive than the absorption measurement. The phase shift features in the active region are clearly visible if the data set is longer than six hours, while it needs a much longer data set to measure the absorption. This advantage may allow us to study the evolution of magnetic fields with the phase maps. Third, the phase information has a better depth resolution than intensity because the phase is determined from the whole time series (Paper II).

The phase maps and the absorption maps are very different. The absorption maps do not show the same structure as the phase maps with simply a higher noise level. The sunspot umbras show up relatively much stronger compared to the other magnetic fields in the phase maps than in the absorption maps. If the phase shift and the acoustic absorption have different dependences on the filling factor of the magnetic fields or on the angle between the magnetic field and the acoustic ray path, then we may be able to measure the field packing or field vector below the surface.

We thank C. Lindsey and the referee D. Braun for their insightful comments. D. Y. C. is grateful to T. Duvall for informative discussions on time-distance helioseismology. D. Y.

C., H. K. C., M. T. S., H. R. C., S. J. Y., and the TON project were supported by NSC of ROC under grants NSC-87-2112-M-007-044, NSC-87-2112-M-007-050, and NSC-87-2112-M-182-003. B. L. was supported by NASA grant NAG5-4941.

REFERENCES

Bogdan, T. J., & Braun, D. C. 1995, in Proc. Fourth *SOHO* Workshop: Helioseismology, ed. V. Domingo et al. (ESA SP-376), 31

Braun, D. C. 1997, ApJ, 487, 447

Braun, D. C., Duvall, T. L., LaBonte, B. J., Jefferies, S. M., Harvey, J. W., & Pomerantz, M. A. 1992, ApJ, 391, L113

Chang, H.-K., Chou, D.-Y., LaBonte, B., & the TON Team. 1997, Nature, 389, 825 (Paper I)

Chen, K.-R., Chou, D.-Y., & the TON Team. 1996, ApJ, 465, 985

Chou, D.-Y., et al. 1995, Sol. Phys., 160, 237

Chou, D.-Y., Chang, H.-K., Sun, M.-T., LaBonte, B., Chen, H.-R., Yeh, S.-J., & the TON Team. 1998, ApJ, submitted (Paper II)

Duvall, T. L., Jr., D'Silva, S., Jefferies, S. M., Harvey, J. W., & Schou, J. 1996, Nature, 379, 235

Duvall, T. L., Jr., Jefferies, S. M., Harvey, J. W., & Pomerantz, M. A. 1993, Nature, 362, 430

Kosovichev, A. G., & Duvall, T. L., Jr. 1998, in Solar Convection and Oscillations and Their Relationship, ed. J. Christensen-Dalsgaard & F. Pijpers (Dordrecht: Kluwer), in press

Lindsey, C., & Braun, D. C. 1997, ApJ, 485, 895